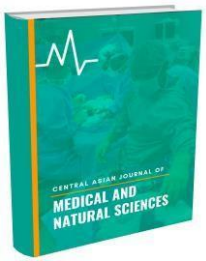

CENTRAL ASIAN JOURNAL OF MEDICAL AND NATURAL SCIENCES
https://cajmns.centralasianstudies.org/index.php/CAJMNS
Volume: 06 Issue: 03 | July 2025 ISSN: 2660-4159

.

Article

A Comparative Study Between Magnesium Ferrite ($Mgfe_2O_4$) and Cobalt Ferrite ($Cofe_2O_4$) in Terms of Optical Properties

Ahmed A. Ahmed[1], Abdullah H. Mohammed[2]

1,2. Department of Physics, College of Education, University, Kirkuk, Iraq
3. Department of Physics College of Education for Women, University of Kirkuk, Iraq

Abstract: This investigation provides a comparative examination of the optical characteristics of magnesium ferrite ($MgFe_2O_4$) and cobalt ferrite ($CoFe_2O_4$), which are two significant spinel ferrites utilized in various applications, including photocatalysis, sensing technologies, and energy-related devices. A range of optical attributes, including the absorption coefficient, refractive index, dielectric function, electrical conductivity, and loss function, were systematically analyzed and contrasted. The findings indicated that both materials exhibit pronounced absorption in the low-energy spectrum, with $MgFe_2O_4$ demonstrating robust absorption in the high-energy range (40-60 eV), whereas $CoFe_2O_4$ revealed considerable absorption in the intermediate energy range (10-30 eV). Additionally, $CoFe_2O_4$ displayed a dielectric response characterized by sharper peaks, suggesting more localized electronic transitions. Moreover, notable distinctions in conductivity and loss function were identified between the two materials. This research substantiates the critical role of chemical composition and crystalline structure in influencing the optical properties of these compounds, thereby enriching the comprehension of their applicability in optical and sensing domains.

Keywords: Magnesium Ferrite, Cobalt Ferrite, Optical Properties, Properties of Magnesium, Sensors

Citation: Ahmed, A. A., Mohammed, A. H. A Comparative Study Between Magnesium Ferrite ($Mgfe_2O_4$) and Cobalt Ferrite ($Cofe_2O_4$) in Terms of Optical Properties. Central Asian Journal of Medical and Natural Science 2025, 6(3), 1339-1349.

Received: 30th May 2025
Revised: 7th Jun 2025
Accepted: 16th Jun 2025
Published: 23rd Jun 2025

1. Introduction

The spinel compounds belonging to the AB2O4 family (including NiFe2O4, $MgFe_2O_4$, and CoFe2O4, among others) hold significant relevance in the domains of materials science and engineering owing to their extensive applicability and exceptional properties. Within the stoichiometric formula of the AB2O4 framework, the components A, B, and O represent the divalent cations, trivalent cations, and divalent anions, respectively. In the configuration of inverse spinel oxides, the A atom is distributed across octahedral sites, while the B atom is uniformly allocated to both tetrahedral and octahedral sites. The spinel ferrites are of considerable interest due to their diverse and remarkable magnetic and electronic characteristics. Notably, CoFe2O4 is distinguished for its exceptional physical and chemical attributes. It demonstrates a high Curie temperature, reduced coercivity, moderate saturation magnetization, elevated magnetic moment, substantial magneto-crystalline anisotropy, a high magnetostrictive coefficient, along with remarkable chemical stability and mechanical hardness [1][2][3][4][5][6][7][8]. The term "Ferrite" is generally attributed to complex oxides that predominantly comprise trivalent iron ions[9].

Conversely, Magnesium ferrite (MgFe2O4) is recognized as one of the paramount materials characterized by a spinel structure. This compound can be classified as an n-type

semiconductor exhibiting a direct bandgap[10]. which renders it suitable for utilization in various applications, including hyperthermia[11]. anode materials [12]. sensors [13]. photocatalysts [14]. and the removal of metal ions [15]. Aside from its straightforward preparation and cost-effectiveness, MgFe2O4 is noted for its high resistivity, as well as its low dielectric and magnetic losses [16]. Spinel ferrites represent significant ceramic materials possessing a variety of intriguing optical, magnetic, structural, and electronic properties. The general representation of spinels is denoted as AB2O4. These spinels exhibit a cubic crystal lattice that conforms to the space group Fd m3, comprising eight formula units per unit cell, which includes thirty-two O anions in a closely packed cubic configuration, in conjunction with twenty-four cations. The classification of spinels is contingent upon the distribution of metal ions across the tetrahedral and octahedral sites, leading to two categories: normal spinel and inverse spinel. In the normal spinel configuration, eight divalent cations occupy the tetrahedral sites, whereas all sixteen trivalent cations are situated in the octahedral sites. Conversely, in the inverse spinel arrangement, the sixteen octahedral sites are evenly shared between eight divalent and eight trivalent cations, while the remaining eight trivalent cations occupy the tetrahedral sites [17]. Predominantly, research concerning $MgFe_2O_4$ has concentrated on empirical investigations, with relatively few studies addressing theoretical aspects. Maensiri et al [18] . reported that $MgFe_2O_4$ possesses a cubic structure typical of normal spinel and is characterized as a soft magnetic n-type semiconducting material. Guo et al [19]. utilized density functional theory (DFT) to conduct the first comprehensive study of various $MgFe_2O_4$ surfaces across three distinct spinel structures: normal, mixed, and inverse. [20]. Based on first-principle calculations and density functional theory (DFT) [21]. In this work we will make a comparison between magnesium ferrite (MgFe2O4) and cobalt ferrite (CoFe2O4) in terms of optical properties. This research aims to conduct a comparative study between magnesium ferrite ($MgFe_2O_4$) and cobalt ferrite ($CoFe_2O_4$) in terms of optical properties, to understand the influence of chemical composition and crystal structure on the optical behavior of these two compounds. These materials are of great importance in technological applications such as solar cells, sensors, photocatalysis, and optoelectronics[22]. Measurements of the optical absorption dimensional coefficient in particular near the main absorption edge, have enhanced the study of optically induced electronic transition[23]. In this study, the effect of varying the addition of magnesium oxide (MgO) to a glass consisting of 65% Na2B4O7 – 35-x% V2O5 – x% MgO, where (x) represents the magnesium oxide produced by conventional melt-quenching technology, was investigated. The structural and optical properties of the glass containing the varying magnesium addition were investigated. X-ray diffraction (XRD) results confirmed the amorphous nature of the samples. The density of the glass network is directly proportional to the amount of magnesium oxide present. Experimental results indicate that the infrared spectra of these glasses are predominantly characterized by the presence of two groups, B2O3 and B2O7. Furthermore, the band shift decreases with increasing MgO concentration in the glass network[24].

2. Materials and Methods

Calculation Model : This models uses in study are based on cobalt ferrite ($CoFe_2O_4$) and magnesium ferrite ($MgFe_2O_4$), both of which crystallize in the spinel structure. These materials exhibit a rhombohedral lattice representation with lattice constants of a = b = c = 5.7441 Å for $CoFe_2O_4$ and a = b = c = 5.9676 Å for $MgFe_2O_4$, and internal angles of $\alpha = \beta = \gamma = 60°$ in both cases. The real and reciprocal lattice vectors for each structure are shown in Table 1. The calculated cell volumes are 134.01 $Å^3$ and 150.27 $Å^3$, with corresponding densities of 5.96 g/cm^3 for $CoFe_2O_4$ and 4.42 g/cm^3 for $MgFe_2O_4$, respectively. These values are consistent with previous experimental and theoretical studies [25]. For both materials, a 2×2×2 supercell is constructed to accurately model the crystal environment, yielding a total of 112 atoms for $MgFe_2O_4$ (based on a 14-atom unit cell) and a corresponding number

for $CoFe_2O_4$ depending on its unit cell composition. In these supercells, the cations are distributed according to the normal spinel configuration, where Mg^{2+}/Co^{2+} occupy tetrahedral (A) sites and Fe^{3+} occupy octahedral (B) sites[26]. To explore the effects of substitutional doping, three configurations are proposed for each ferrite. In Model I, a dopant atom replaces an Fe^{3+} ion at a central B site. In Model II, the dopant is located at a B site near the cell boundary. In Model III, the substitution occurs at a B site adjacent to an A-site cation (Mg or Co), potentially affecting local electronic and magnetic interactions. The atomic structures of these models are illustrated in Figures 1(b)–1(d). All structures are fully relaxed using appropriate convergence criteria before proceeding with further electronic, magnetic, and thermodynamic property calculations[27].

Calculation Method: The computational analysis was executed utilizing the first-principles approach grounded in density functional theory (DFT)[28]. The geometric configuration, energy states, band structure, Mulliken population analysis, and the three-dimensional optical characteristics of the ($MgFe_2O_4$) and ($CoFe_2O_4$) complexes were derived employing the CASTEP software package[26]. The ultra-soft pseudopotential (USPP)[29]. was implemented to address the interactions between ionic cores and electrons, while the Perdew–Burke–Ernzerhof (PBE) functional[30]. of the generalized gradient approximation (GGA) was employed to account for the exchange-correlation energy among electrons. We established the plane wave truncation energy at 340 eV and the energy convergence precision at 1.0×10−6 eV/atom. We designated (Mg: $1s^2\ 2s^2\ 2p^6\ 3s^2$, Fe: $3d^6\ 4s^2$, and O: $1s^2\ 2s^2\ 2p^4$) and (Co: $3d^7\ 4s^2$, Fe: $3d^6\ 4s^2$, O: $1s^2\ 2s^2\ 2p^4$) as valence electrons, with all other orbital electrons classified as core electrons for the computational procedure. The K-point path was specified as

Γ(0, 0, 0) ⟶ K(1,1,1). The 5×5×5 MonkhorstandPack[31]. The total number of bands included in the optical calculations was 92. The optical properties were computed within the independent particle approximation, and the dielectric function was obtained using the linear response method[32].

The relationship between the wavelength of light (λ) and the dispersion of the refractive index (n) is expressed as follows.

$$\mathbf{n = A+\frac{B}{\lambda^2} + \frac{C}{\lambda^4}} \quad \text{.....(1)}$$

Where A, B, and C are special constants dependent on the material.

$$\boldsymbol{\alpha(\omega) = \frac{2\omega k(\omega)}{c}} \quad \text{.....(2)}$$

$\alpha(\omega)$: $Absorption\ coefficient$

c : Speed of light in vacuum

ω : angular frequency of incident light

K(ω): $Extinction\ coefficient$

$$R(w) = \frac{(n-1)^2+K^2}{(n+1)^2+K^2} \quad \text{.....(3)}$$

n: Refractive Index

k: Extinction Coefficient

R(ω) : Reflectivity as a function of angular frequency

3. Results and Discussion

Optical properties of the compound (MgFe2O4)

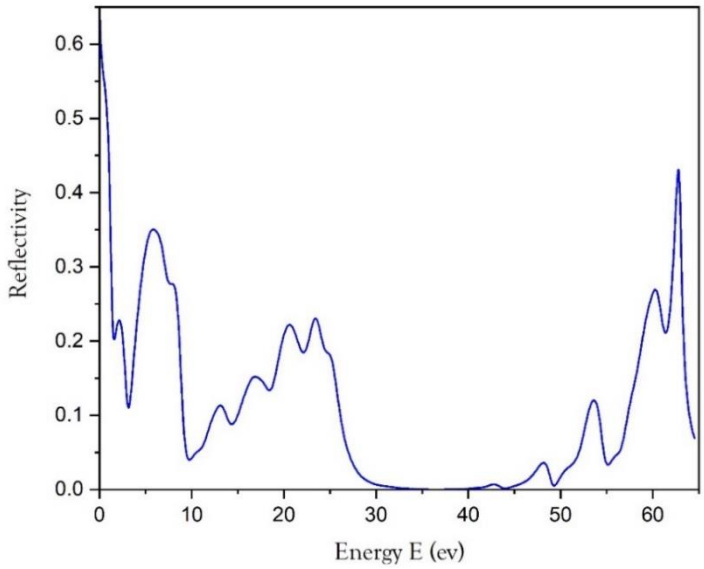

Figure 1. This figure represents the reflectivity as a function of energy for the compound ($MgFe_2O_4$).

Illustrates Figure 1the relationship between reflectivity and energy in electron volts. The curve represents the response of a material to electromagnetic radiation in a specific energy range, which often reflects the properties of the material's electronic structure. A significant decrease in reflectivity is observed at around (30 ev), indicating the presence of a strong absorption point at this energy. At lower energies (>10 ev), the reflectivity begins to rise and then fluctuates, which may be related to the material's electronic structure, plasmon effects, or electronic excitations. However, at higher energies (<50ev), a sharp increase in reflectivity is observed, along with prominent peaks, indicating the presence of electronic transitions.

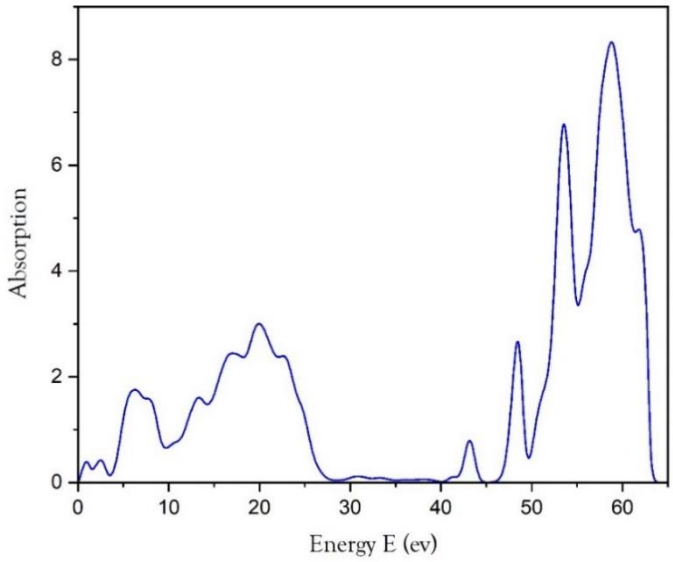

Figure 2. Represents the absorption coefficient as a function of energy for the compound ($MgFe_2O_4$).

The figure shows the relationship between absorption and energy in electron volts. It is clear from the figure that there are three energy levels. The first: where absorption is weak and ranges between (0-10ev) and this is Due to electron transitions between

conduction and valence energies which are affected by the electronic configuration of the iron and magnesium ions. The second: are the peaks that range between (10-30ev) and indicate electron transitions within the iron ions. The third: is the one with high absorption, ranging between (40-60ev) which indicates possible ionization processes where the electrons gain sufficient energy to escape from the valence band.

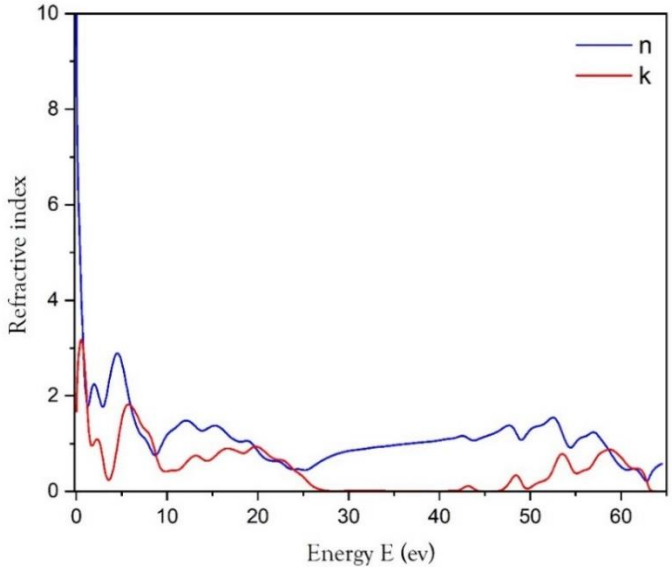

Figure 3. The refractive index in this figure is represented as a function of energy for the compound ($MgFe_2O_4$).

This figure illustrates The relationship between absorption coefficient (k) and refractive index (n) . It is clear from this figure that (n,k) increases at low energies, indicating a strong absorption band. In addition, the decrease in (k) at high energies makes the material more transparent to these frequencies. The electronic structure of a material is related to the current fluctuation.

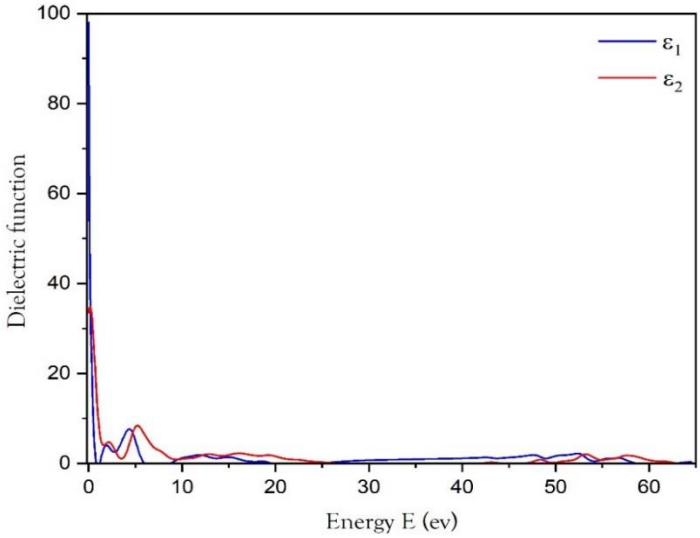

Figure 4. This figure represents the dielectric function of the energy function, for the compound ($MgFe_2O_4$).

This figure illustrates three things. First, (ε_1) appears with a high value at low energies and then decreases rapidly, indicating that the material has a good dielectric response. Second, (ε_2)appears with a sharp peak at low energies as well, indicating the presence of strong electronic transitions. As the energy increases, the absorption fades. Third, (ε_1.ε_2) values become very small when the energy level ranges between (20-30ev) and indicating that the material no longer absorbs photons well.

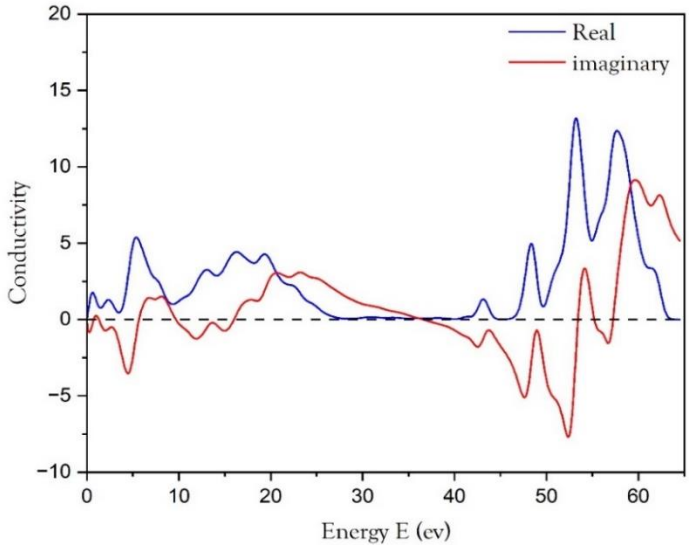

Figure 5. This figure represents the conductivity as a function of energy, for the compound ($MgFe_2O_4$).

This figure shows the presence of three energy levels. When the energy is low between (0-10ev) the intrinsic conductivity will appear with small positive values, indicating the beginning of weak electron transitions. When the energy is intermediate between (10-30ev) we observe a gradual increase in the intrinsic conductivity, meaning that more electrons are being stimulated towards the conduction band. At high energy levels, greater than 40, the intrinsic conductivity increases significantly, indicating the presence of electron transitions.

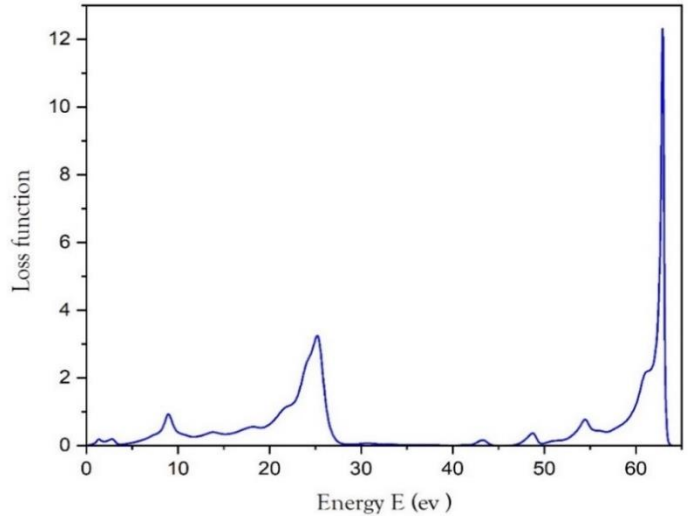

Figure 6. The loss function is considered as a function of energy, for the compound ($MgFe_2O_4$)

This figure illustrates the spectral loss function, which expresses the extent of energy loss of electrons during their interaction with the materialIt is intrinsically associated with the plasmonic phenomena and the optical characteristics of the substance, and there exist various energy states. The spectral loss function is related to the imaginary part of the dielectric function such that the peaks occur at energies at which a large change occurs in the material's response to electromagnetic waves. The plasmon energy can be extracted from the principal peak position in the loss function.

Optical properties of the compound ($CoFe_2O$)

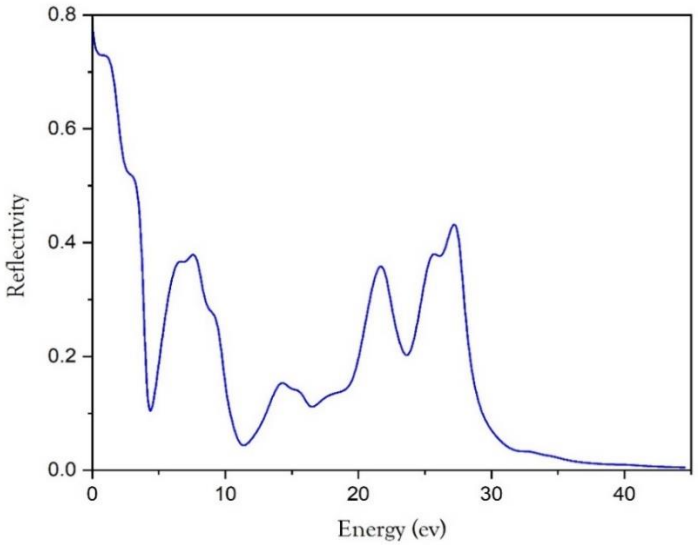

Figure 7. The absorption coefficient as a function of energy, for the compound ($CoFe_2O_4$).

This figure shows that reflectivity is high at low energies, indicating that the material reflects most of the incident light at these energies. After that, we observe a sharp decrease in reflectivity, indicating the onset of optical absorption due to electronic transitions. There are also multiple peaks at intermediate energies, indicating electronic response.

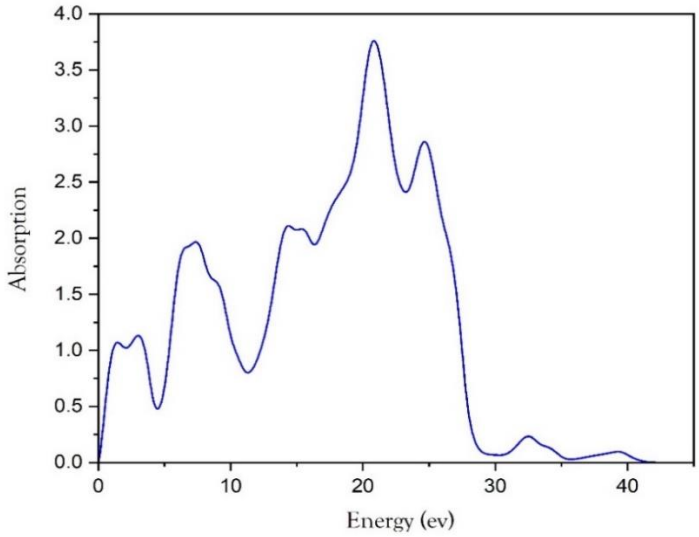

Figure 8. The absorption coefficient as a function of energy, for the compound ($CoFe_2O_4$).

The figure shows three energy levels. The first has medium absorption, ranging (0-10ev), due to electron transitions within the iron ions. The second has high absorption, ranging (10-30ev), indicating potential ionization processes in which electrons gain sufficient energy to escape the valence band. The third has low absorption, ranging (30-40ev) Due to electron transitions between conduction and valence energies.

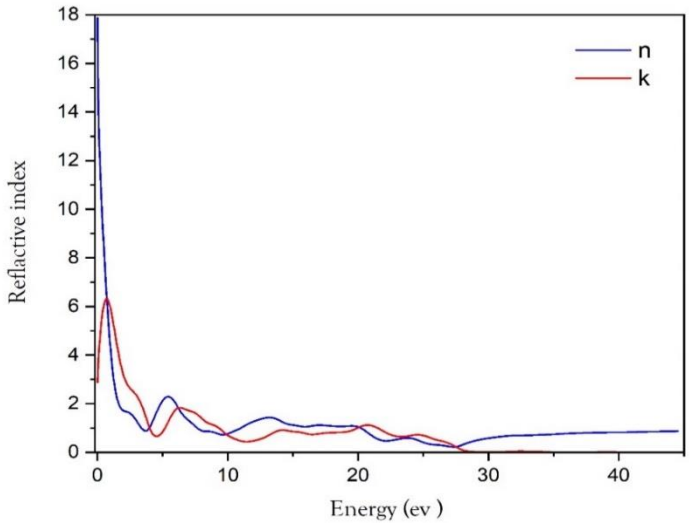

Figure 9. Represents the refractive index as a function of energy for the compound ($CoFe_2O_4$).

This figure illustrates the relationship between the refractive index (n) and the absorption coefficient (k). It is clear from this figure that (n,k) increases at low energies, indicating a strong absorption band. In addition, the decrease in (k) at high energies makes the material more transparent to these frequencies. The current fluctuation is related to the electronic structure of the material.

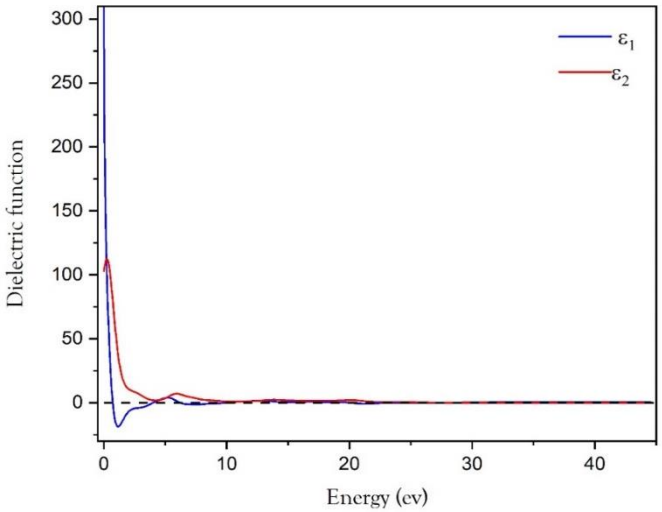

Figure 10. Represents the dielectric function as a function of energy for the compound ($CoFe_2O_4$).

This figure illustrates three things. First, (ε_1) appears with a high value at low energies and then decreases rapidly, indicating that the material has a good dielectric response. Second, (ε_2) appears with a sharp peak at low energies as well, indicating the presence of strong electronic transitions. As the energy increases, the absorption fades. Third, (ε_1.ε_2) values become very small when the energy level ranges between (20-30ev) and indicating that the material no longer absorbs photons well.

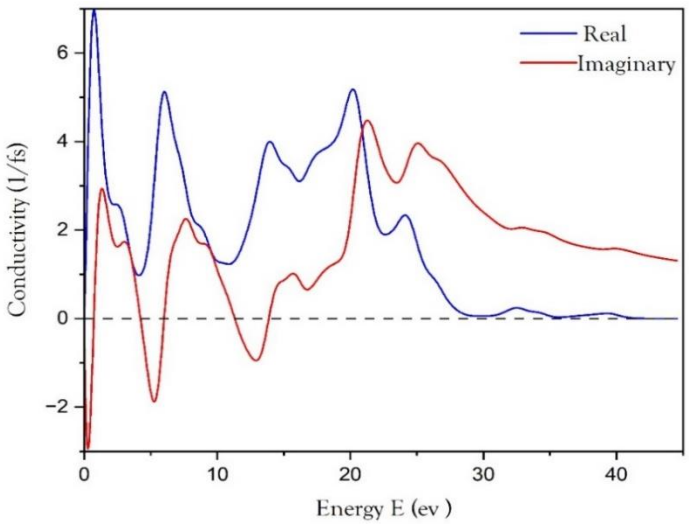

Figure 11. Represents the conductivity as a function of energy for the compound($CoFe_2O_4$).

The figure shows that the peaks in conductivity represent electronic transitions between different energy levels within the material. There are also dips and fluctuations that indicate interference or scattering effects resulting from the material's structure. Conductivity is most stable at high energies, which means that most of the important effects occur at low and intermediate energies. Finally, we note the presence of negative values in the imaginary part, which may indicate unconventional absorption effects and complex responses of the electronic structure.

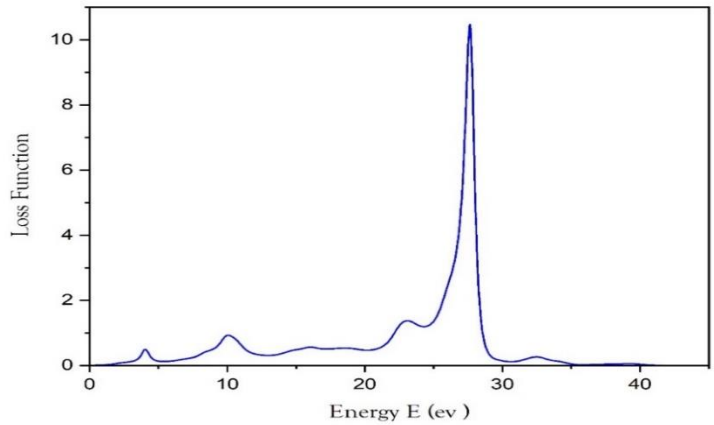

Figure 12. Represents the loss function as a function of energy for the compound($CoFe_2O_4$).

This figure illustrates the loss function, which expresses the extent of energy loss of electrons during their interaction with the material. It is directly related to the plasmons and optical properties of the material, and there are different energy levelsThe loss function is related to the imaginary part of the dielectric function and when there is a large change in the response of the material to electromagnetic waves, peaks occur at these energies.. The plasmon energy can be extracted from the principal peak position in the loss function.

4. Conclusion

In summary, this comparative analysis of magnesium ferrite ($MgFe_2O_4$) and cobalt ferrite ($CoFe_2O_4$) has yielded significant insights into the optical characteristics of these two spinel ferrites, which are essential for a myriad of technological applications. Both substances demonstrate unique optical behaviors, shaped by their respective chemical compositions and crystalline structures. $MgFe_2O_4$ exhibits enhanced absorption at elevated

energies, particularly within the 40-60 eV range, indicative of ionization phenomena, whereas $CoFe_2O_4$ reveals considerable absorption at intermediate energy levels (10-30 eV), linked to electronic transitions among the Fe^{3+} and Co^{2+} ions. The dielectric and refractive index characteristics of both materials imply favorable dielectric responses at lower energies, with $CoFe_2O_4$ exhibiting more pronounced transitions, suggesting an increased localization of electronic states. Moreover, the analyses of conductivity and loss functions indicate that $CoFe_2O_4$ experiences greater fluctuations at intermediate energies, pointing to more intricate electronic interactions. These observations emphasize the necessity of comprehending the material's composition and structure in optimizing their optical properties for targeted applications such as sensors, optoelectronics, and energy harvesting devices. Both $MgFe_2O_4$ and $CoFe_2O_4$ possess distinct optical attributes rendering them suitable for diverse technological applications, with $MgFe_2O_4$ being particularly advantageous for applications requiring high-energy absorption and $CoFe_2O_4$ exhibiting potential for sensor and optoelectronic applications due to its expansive absorption range and unique dielectric properties.

REFERENCES

[1] P. C. R. Varma, R. S. Manna, D. Banerjee, M. R. Varma, K. G. Suresh, and A. K. Nigam, "Magnetic properties of CoFe2O4 synthesized by solid state, citrate precursor and polymerized complex methods: A comparative study," *J. Alloys Compd.*, vol. 453, no. 1–2, pp. 298–303, 2008.

[2] A. Hossain, M. S. I. Sarker, M. K. R. Khan, F. A. Khan, M. Kamruzzaman, and M. M. Rahman, "Structural, magnetic, and electrical properties of sol–gel derived cobalt ferrite nanoparticles," *Appl. Phys. A*, vol. 124, pp. 1–7, 2018.

[3] A. Lisfi and C. M. Williams, "Magnetic anisotropy and domain structure in epitaxial CoFe2O4 thin films," *J. Appl. Phys.*, vol. 93, no. 10, pp. 8143–8145, 2003.

[4] C. N. Chinnasamy *et al.*, "Unusually high coercivity and critical single-domain size of nearly monodispersed CoFe 2 O 4 nanoparticles," *Appl. Phys. Lett.*, vol. 83, no. 14, pp. 2862–2864, 2003.

[5] H. Zheng *et al.*, "Multiferroic batio3-cofe2o4 nanostructures," *Science (80-.).*, vol. 303, no. 5658, pp. 661–663, 2004.

[6] R. V Chopdekar and Y. Suzuki, "Magnetoelectric coupling in epitaxial CoFe2O4 on BaTiO3," *Appl. Phys. Lett.*, vol. 89, no. 18, 2006.

[7] H. Zheng *et al.*, "Self-assembled growth of BiFeO3–CoFe2O4 nanostructures," *Adv. Mater.*, vol. 18, no. 20, pp. 2747–2752, 2006.

[8] I. H. Gul, A. Z. Abbasi, F. Amin, M. Anis-ur-Rehman, and A. Maqsood, "Structural, magnetic and electrical properties of Co1− xZnxFe2O4 synthesized by co-precipitation method," *J. Magn. Magn. Mater.*, vol. 311, no. 2, pp. 494–499, 2007.

[9] M. H. A. Albayati and S. M. A. Ridha, "A study on the dielectric properties of La doped nickel ferrite".

[10] W. Fan *et al.*, "Fabrication of MgFe2O4/MoS2 heterostructure nanowires for photoelectrochemical catalysis," *Langmuir*, vol. 32, no. 6, pp. 1629–1636, 2016.

[11] M. Bagheri, M. A. Bahrevar, and A. Beitollahi, "Synthesis of mesoporous magnesium ferrite (MgFe2O4) using porous silica templates," *Ceram. Int.*, vol. 41, no. 9, pp. 11618–11624, 2015.

[12] Y. Yin *et al.*, "Hollow spheres of MgFe2O4 as anode material for lithium-ion batteries," *Scr. Mater.*, vol. 110, pp. 92–95, 2016.

[13] R. V Godbole, P. Rao, P. S. Alegaonkar, and S. Bhagwat, "Influence of fuel to oxidizer ratio on LPG sensing performance of MgFe2O4 nanoparticles," *Mater. Chem. Phys.*, vol. 161, pp. 135–141, 2015.

[14] K. Tezuka, M. Kogure, and Y. J. Shan, "Photocatalytic degradation of acetic acid on spinel ferrites MFe2O4 (M= Mg, Zn, and Cd)," *Catal. Commun.*, vol. 48, pp. 11–14, 2014.

[15] V. Srivastava, Y. C. Sharma, and M. Sillanpää, "Application of nano-magnesso ferrite (n-MgFe2O4) for the removal of Co2+ ions from synthetic wastewater: kinetic, equilibrium and thermodynamic studies," *Appl. Surf. Sci.*, vol. 338, pp. 42–54, 2015.

[16] M. Tada, T. Kanemaru, T. Hara, T. Nakagawa, H. Handa, and M. Abe, "Synthesis of hollow ferrite nanospheres for biomedical applications," *J. Magn. Magn. Mater.*, vol. 321, no. 10, pp. 1414–1416, 2009.

[17] J. Yao, Y. Li, X. Li, and X. Zhu, "First-principles study of the geometric and electronic structures of zinc ferrite with vacancy defect," *Metall. Mater. Trans. A*, vol. 47, pp. 3753–3760, 2016.

[18] S. Maensiri, M. Sangmanee, and A. Wiengmoon, "Magnesium ferrite (MgFe 2 O 4) nanostructures fabricated by electrospinning," *Nanoscale Res. Lett.*, vol. 4, pp. 221–228, 2009.

[19] H. H. Kora, M. Taha, A. Abdelwahab, A. A. Farghali, and S. I. El-Dek, "Effect of pressure on the geometric, electronic structure, elastic, and optical properties of the normal spinel MgFe2O4: a first-principles study," *Mater. Res. Express*, vol. 7, no. 10, p. 106101, 2020.

[20] H. Guo *et al.*, "Essential role of spinel MgFe2O4 surfaces during discharge," *J. Electrochem. Soc.*, vol. 167, no. 9, p. 90506, 2020.

[21] I. Z. A. Hassan and S. M. Nayif, "Computational Study of the Effect of Adsorbed Lithium on Solid State Hydrogen Storage Capacity of Pristine and Boron Doped Graphene," *Kirkuk J. Sci.*, vol. 15, no. 4, 2020.

[22] S. Chikazumi and C. D. Graham, *Physics of ferromagnetism*, no. 94. Oxford university press, 1997.

[23] N. F. Mott and E. A. Davis, *Electronic processes in non-crystalline materials*. OUP Oxford, 2012.

[24] H. M. Ahmed and M. J. Ali, "Effect of V 2 O 5 – MgO Addition on Some Structural and Physical Properties of Na 2 B 4 O 7," vol. 21, no. 1, pp. 75–78, 2025.

[25] N. Thomas, P. V Jithin, V. D. Sudheesh, and V. Sebastian, "Magnetic and dielectric properties of magnesium substituted cobalt ferrite samples synthesized via one step calcination free solution combustion method," *Ceram. Int.*, vol. 43, no. 9, pp. 7305–7310, 2017, doi: https://doi.org/10.1016/j.ceramint.2017.03.031.

[26] S. Akhtar, A. Hussain, S. Noreen, N. Bibi, M. Bilal Tahir, and J. Ur Rehman, "A comparative DFT study of MgFe2O4 and MnFe2O4 spinel ferrites at various pressures to investigate the structural, mechanical, electronic, magnetic and optical properties for multifunctional applications," *Comput. Theor. Chem.*, vol. 1235, p. 114546, 2024, doi: https://doi.org/10.1016/j.comptc.2024.114546.

[27] T. Rui, Y. Lan, C. Li, H. Zhang, and X. Liu, "First principle investigation of Cr doping effect on the stability of NiFe2O4," *AIP Adv.*, vol. 15, no. 1, 2025.

[28] S. Caliskan, M. A. Almessiere, A. Baykal, and Y. Slimani, "A first principles study on electronic structure, magnetic and optical characteristics of Se doped CoNiFe2O4 spinel ferrites," *Comput. Mater. Sci.*, vol. 226, p. 112243, 2023.

[29] K. F. Garrity, J. W. Bennett, K. M. Rabe, and D. Vanderbilt, "Pseudopotentials for high-throughput DFT calculations," *Comput. Mater. Sci.*, vol. 81, pp. 446–452, 2014.

[30] Y. Didi *et al.*, "Computational insights into spin-polarized density functional theory applied to actinide-based perovskites $XBkO_3$ (X= Sr, Ra, Pb)," *Sci. Rep.*, vol. 15, no. 1, p. 87, 2025.

[31] C. A. P. Liberato, S. R. Jáuregui-Rosas, and A. V Gil Rebaza, "Structural and Magnetic Ground State of the Spinel CoFe2O4: A Density Functional Theory Study," *J. Supercond. Nov. Magn.*, pp. 1–7, 2024.

[32] Q. Luan, C.-L. Yang, M.-S. Wang, and X.-G. Ma, "First-principles study on the electronic and optical properties of WS2 and MoS2 monolayers," *Chinese J. Phys.*, vol. 55, no. 5, pp. 1930–1937, 2017.